



Preferential Formation of Benzo[a]pyrene Adducts at Lung Cancer Mutational Hotspots in P53
Author(s): Mikhail F. Denissenko, Annie Pao, Moon-shong Tang, Gerd P. Pfeifer

Reviewed work(s):

Source: *Science*, New Series, Vol. 274, No. 5286 (Oct. 18, 1996), pp. 430-432

Published by: [American Association for the Advancement of Science](#)

Stable URL: <http://www.jstor.org/stable/2891966>

Accessed: 02/12/2011 16:54

Your use of the JSTOR archive indicates your acceptance of the Terms & Conditions of Use, available at
<http://www.jstor.org/page/info/about/policies/terms.jsp>

JSTOR is a not-for-profit service that helps scholars, researchers, and students discover, use, and build upon a wide range of content in a trusted digital archive. We use information technology and tools to increase productivity and facilitate new forms of scholarship. For more information about JSTOR, please contact support@jstor.org.



American Association for the Advancement of Science is collaborating with JSTOR to digitize, preserve and extend access to *Science*.

<http://www.jstor.org>

nipause neurons in the brainstem, which gate saccade initiation, cease discharging 8 to 10 ms before saccade initiation [J. A. Buttner-Ennever, B. Cohen, M. Pause, W. Fries, *J. Comp. Neurol.* **267**, 307 (1988)], and the transduction time from FEF movement cells to the omnipause cells is around 4 ms [M. A. Segraves, *J. Neurophysiol.* **68**, 1967 (1992)]. According to these times, then, the FEF cannot influence saccade initiation later than 12 to 14 ms before the movement begins. Also, the modal time of burst onset within FEF movement cells is 10 ms before saccade initiation (7). Finally, the minimum latency of the saccades evoked by electrical stimulation of FEF is around 20 ms [C. J. Bruce, M. E. Goldberg, C. Bushnell, G. B. Stanton, *J. Neurophysiol.* **54**, 714 (1985)]. The results of the analysis we report did not change when the level of activation was measured 20 to 30 or 0 to 10 ms before saccade initiation.

13. All trials for a neuron were rank ordered by reaction time and were split into equal groups containing at least 10 trials on the basis of reaction time. Thus, the first group consisted of the trials with the 10 shortest reaction times, and so on. The number of reaction-time groups varied across cells because of different trial numbers. If the total number of no-signal trials was less than 50, the number of trials in each saccade latency group was set so that five saccade latency groups were generated.
14. An algorithm was applied to each trial to identify periods of activity in which more spikes occurred than would be predicted from a random Poisson process having the overall average rate of the trial [C. R. Legéndy and M. Salzman, *J. Neurophysiol.* **53**, 926 (1985); (7)]. For each group of reaction time trials, the mode of the distribution of response beginning times was determined.
15. There were a total of 190 saccade latency groups across all 25 cells. The average r^2 of the linear regression on the activation function was 0.79 (minimum = 0.34, maximum = 0.99). A Durbin-Watson test for autocorrelation of the residuals provided another test of the goodness of fit of the neural activation function with a line. For only 12 of the 190 saccade latency groups was there a significant autocorrelation between the residuals. The fact that a linear function provided such a good fit to the activation function is further evidence against the variable threshold model that posits a decelerating accumulator function.
16. The magnitude of the lateralized readiness potential at movement initiation does not vary with reaction time [G. Gratton, M. G. H. Coles, E. Sirevaag, C. W. Eriksen, E. Donchin, *J. Exp. Psychol. Human Percept. Perform.* **14**, 331 (1988)], and the lateralized readiness potential does not reach a critical threshold level in signal-inhibit trials [R. DeJong, M. G. H. Coles, G. D. Logan, G. Gratton, *ibid.* **16**, 164 (1990)].
17. The reaction time on the i th simulation trial was $RT_i = t_{ON} + (A'/r)_i$, where t_{ON} is the onset latency of the cell, A' is the threshold activation level, and r is the rate of growth of the activation function. The onset latency of the growth of the accumulator (t_{ON}), specified by the Poisson spike-train analysis, was held constant across simulated trials. The trigger threshold (A') was held constant across simulated trials at the average threshold activation measured across all reaction time groups collected for that cell (for example, Fig. 3D). The rate of growth of the simulated accumulator function (r) was selected on each simulated trial from a Gaussian distribution. The mean and SD of the sampled Gaussian distribution were derived from the rates of growth of the activation functions across the reaction-time groups collected for that cell (for example, Fig. 3E).
18. We thank O. Armstrong and D. King for assistance with data acquisition and analysis and N. Bichot, R. Blake, R. Carpenter, K. Cave, J. Kaas, J. Lappin, and K. Thompson for helpful discussion and comments on the manuscript. Supported by National Institute of Mental Health grants F31-MH11178 to D.P.H. and R01-MH55806 to J.D.S. and National Eye Institute (of NIH) grant P30-EY08126 to the Vanderbilt Vision Research Center. J.D.S. is a Kennedy Center Investigator.

2 July 1996; accepted 23 August 1996

Preferential Formation of Benzo[a]pyrene Adducts at Lung Cancer Mutational Hotspots in *P53*

Mikhail F. Denissenko, Annie Pao, Moon-shong Tang,*
Gerd P. Pfeifer*

Cigarette smoke carcinogens such as benzo[a]pyrene are implicated in the development of lung cancer. The distribution of benzo[a]pyrene diol epoxide (BPDE) adducts along exons of the *P53* gene in BPDE-treated HeLa cells and bronchial epithelial cells was mapped at nucleotide resolution. Strong and selective adduct formation occurred at guanine positions in codons 157, 248, and 273. These same positions are the major mutational hotspots in human lung cancers. Thus, targeted adduct formation rather than phenotypic selection appears to shape the *P53* mutational spectrum in lung cancer. These results provide a direct etiological link between a defined chemical carcinogen and human cancer.

Lung cancer is currently the leading cause of cancer death in the United States and is also the most common type of tumor worldwide. Tobacco smoking is the single most important risk factor for lung cancer. Among the many components of cigarette smoke, polycyclic aromatic hydrocarbons are strongly implicated as causative agents in the development of these cancers (1). Benzo[a]pyrene, which occurs in amounts of 20 to 40 ng per cigarette, is by far the best studied of these compounds and is one of the most potent mutagens and carcinogens known. The compound requires metabolic activation to become the ultimate carcinogenic metabolite, BPDE [(±)-anti-7β,8α-dihydroxy-9α,10α-epoxy-7,8,9,10-tetrahydrobenzo[a]pyrene], which binds to DNA and forms predominantly covalent (+) trans adducts at the N2 position of guanine (2).

About 60% of human lung cancers contain mutations in the *P53* tumor suppressor gene (3). The *P53* mutation database (4) includes more than 500 entries of sequenced *P53* mutations for lung cancer. There is a large percentage of G to T transversion mutations in these tumors. Such mutations are hallmarks of mutagenesis involving certain types of polycyclic aromatic hydrocarbons, including BPDE (5), but they can also be induced by other agents, including oxidative DNA damage (6). The distribution of mutations along the *P53* gene in lung cancer is nonrandom but rather is characterized by several mutational hotspots, in particular, at codons 157, 248, and 273 (Fig. 1), which correspond to ami-

no acids within the DNA binding domain of p53. Codon 157 is a mutational hotspot specific for lung cancer and does not occur as a hotspot in any other cancer, but the other two codons are affected in many different tumor types (3, 7). The majority of lung cancer mutations at these three codon positions are G to T transversions (4).

To investigate the relation between BPDE adduct formation and *P53* mutations, we mapped the distribution of BPDE adducts along the *P53* gene using a modification of the ligation-mediated polymerase chain reaction (LMPCR) (8). HeLa cells were treated with various concentrations of BPDE (9), and DNA was isolated and cleaved at the sites of modified bases with the UvrABC nuclease complex from *Escherichia coli* (10). UvrABC makes a dual incision 5' and 3' to the adducted base, and the 3' incision occurs specifically at the fourth nucleotide position 3' to a BPDE adduct (11). These break positions can then be visualized by LMPCR in which *P53*-specific oligonucleotide primers were used (12, 13). Figure 2A shows an analysis of the upper (nontranscribed) DNA strand of exon 5. One of the strongest BPDE-derived signals along the exon is seen at codon 157, which is one of the major mutational hotspots in lung cancer. In exon 7, the two guanine positions within the frequently mutated codon 248 are the preferred targets for BPDE adduct formation (Fig. 2B). The same is true for exon 8, where the strongest signal corresponds to a BPDE adduct at the guanine within the mutational hotspot codon 273 (Fig. 2C).

To analyze a cell type that is more representative of the target cell population during lung tissue transformation, we performed similar experiments with normal human bronchial epithelial cells (14). The BPDE adduct patterns were generally simi-

M. F. Denissenko and G. P. Pfeifer, Department of Biology, Beckman Research Institute of the City of Hope, Duarte, CA 91010, USA.
A. Pao and M.-s. Tang, M. D. Anderson Cancer Center, University of Texas, Science Park, Smithville, TX 78957, USA.

*To whom correspondence should be addressed.

lar between HeLa cells and normal bronchial cells. Most important, the adduct hotspots were the same in the bronchial epithelial cells (Fig. 3).

To test whether the sequence specificity is related to chromatin structure, we compared the adduct pattern in BPDE-treated HeLa cells with the pattern in BPDE-treated isolated genomic DNA. The two patterns were almost identical (15), which excludes chromatin structure as a major modulating factor for the cell types analyzed. It should be noted that the histogenesis of the different types of lung cancer is incompletely understood. Therefore, it is important that a similar adduct pattern was seen in three different cell types: HeLa cells (Fig. 2), bronchial cells (Fig. 3), and normal human fibroblasts (15). This pattern does not appear to be greatly modified by cell type-specific chromatin structure, which suggests that the same adduct pattern is likely to be present in the unidentified target cells for lung tissue transformation. Strong selectivity of BPDE binding at guanine positions in codons 157, 248, and 273 was not observed in previous experiments in which a DNA polymerase fingerprint assay was used to detect adducts formed in carcinogen-treated plasmid DNA (16). The apparent discrepancies between our findings and those of this previous study could be due to different methylation patterns in *E. coli* versus human DNAs; however, the discrepancies may also arise from differences in specificity and sensitivity of the detection method.

The BPDE adduct hotspots are on the nontranscribed DNA strand, which is expected to be repaired relatively inefficiently, according to the concept of transcription-coupled repair (17, 18). A strand bias in repair is consistent with the majority (>90%) of G to T mutations in lung cancer attributable to guanines on the nontranscribed strand (3, 4).

Codon 179, which is also frequently mutated in lung tumors, is not a strong target for BPDE adduct formation (Fig. 2A). However, this codon does not contain a guanine on the nontranscribed strand, and the majority of mutations are A to G transitions at the second codon base (4). BPDE binds to guanine 20 times more efficiently than to adenine; thus, it is likely that these mutations are caused by another mutagenic component of cigarette smoke. Pronounced adduct formation was observed at codon 267 (Figs. 2C and 3C), for which there is only one mutation entry in the *P53* database. Here, the most strongly adducted base corresponds to the third codon position (CGG), and a mutation would not produce an amino acid change.

It has been generally assumed that *P53*

cancer mutations occur frequently at specific codons because they are selected for in the cell transformation process. One possibility is that mutational hotspot codons are sites of preferred gain of function mutations or sites that are most important for tumor suppressor function of the protein. The presence of mutational hotspots has been correlated with crystal structure data obtained from a p53 protein-DNA complex (19). The most frequently mutated amino acids (residues 248 and 273) contact DNA directly, whereas some of the other com-

monly mutated amino acids contribute to stabilization of the protein (19). In lung cancers, mutations in the *P53* gene are found at more than 100 different sequence positions (Fig. 1), and it is likely that all of these mutations can provide a growth advantage. These results, together with our current finding that *P53* mutation hotspots 157, 248, and 273 act as selective BPDE binding sites, suggest that *P53* mutation hotspots are preferential targets for DNA-damaging agents and that selection may not necessarily play a major role in the occur-

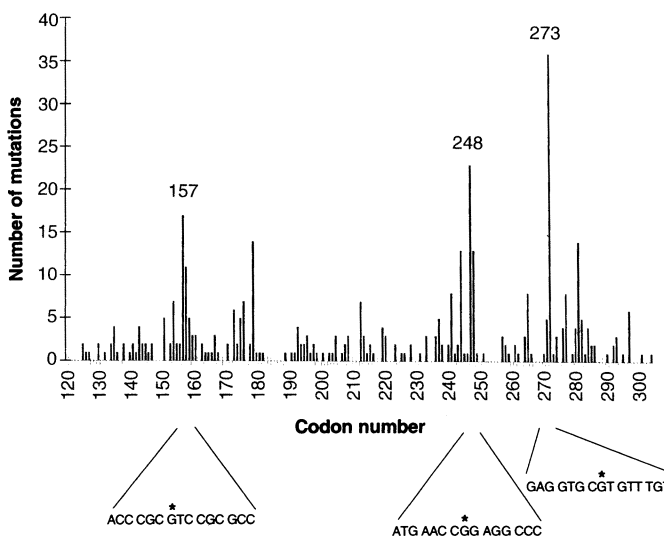


Fig. 1. Frequency of *P53* mutations in lung cancer by codon position. Numbers were obtained from the *P53* database (4). Radon-associated lung cancers and cancers from nonsmokers were excluded. The sequences surrounding the mutational hotspot codons 157, 248, and 273 are indicated. The asterisks mark the mutated Gs within these codons.

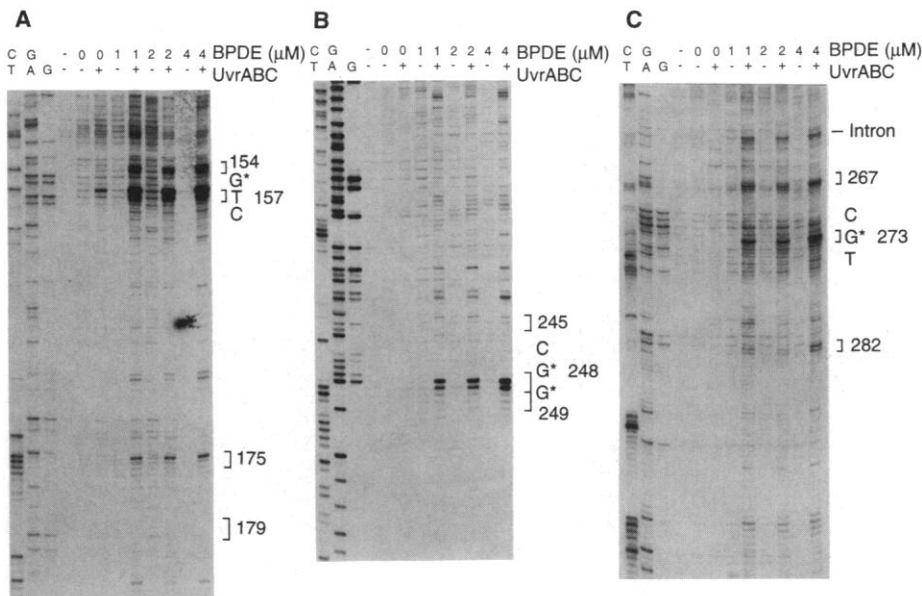


Fig. 2. Distribution of BPDE adducts along *P53* exons in HeLa cells. Cells were treated with various concentrations of BPDE, and the distribution of adducts in *P53* was determined after cleavage with UvrABC nuclease and LMPCR (11, 12). Adduct-specific bands migrate four nucleotide positions faster than the corresponding bands in the Maxam-Gilbert sequencing ladders (left three lanes). Some bands in the sequencing lanes are absent because 5-methylcytosines are not cleaved (13). (A) Exon 5, nontranscribed strand. (B) Exon 7, nontranscribed strand. (C) Exon 8, nontranscribed strand. Brackets indicate the positions of selected *P53* codons. Asterisks mark the strongly modified G positions within codons 157, 248, and 273.

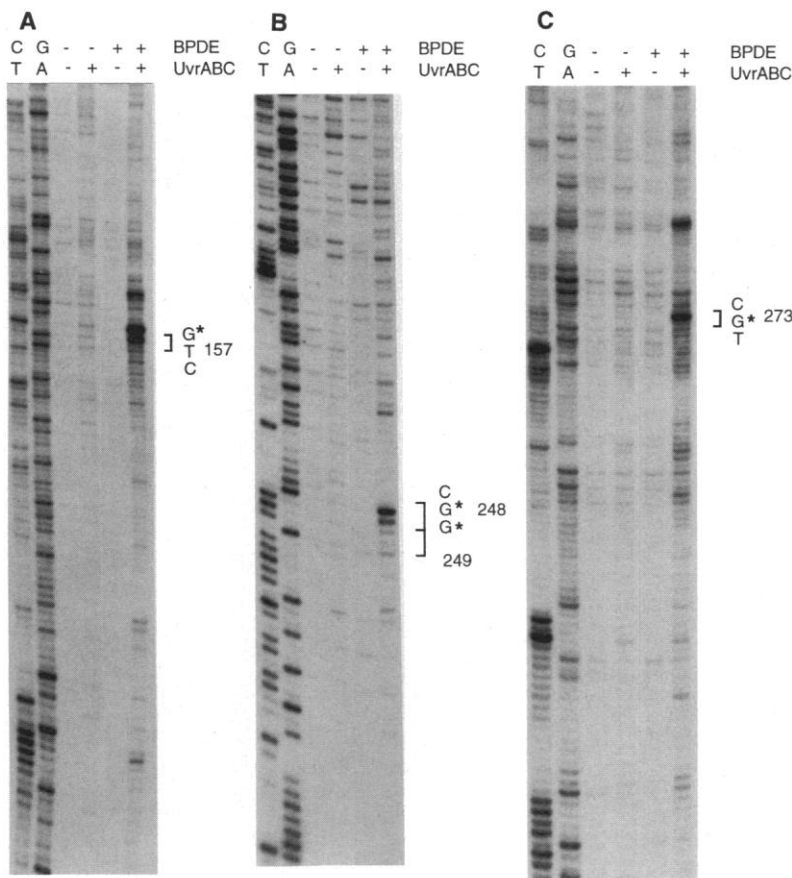


Fig. 3. Distribution of BPDE adducts along *P53* exons in bronchial epithelial cells. Cells were treated with 4 μ M of BPDE for 30 min, and the distribution of adducts in *P53* was determined after cleavage with UvrABC nuclease and LMPCR. (A) Exon 5, nontranscribed strand. (B) Exon 7, nontranscribed strand. (C) Exon 8, nontranscribed strand. Asterisks mark the strongly modified G positions within codons 157, 248, and 273.

rence of mutations at these sites.

It is also of interest that two of the adduct hotspots (at codons 248 and 273) are at positions that are common mutational sites not only in lung cancer but also in many other cancers. Almost all of the adduct hotspots were at CpG dinucleotides, although not all CpG sites were strong binding sites for BPDE. Because the CpG sites in the *P53* gene are methylated in every human tissue or cell type examined (13, 20), the preferentially adducted sequence in vivo is 5-methyl-CpG. Whether selective DNA damage also plays a role in the frequent occurrence of transition mutations at specific CpG codons (codons 175, 245, 248, 273, and 282) remains to be determined.

The coincidence of mutational hotspots

and adduct hotspots suggests that benzo[a]pyrene metabolites or structurally related compounds are involved in transformation of human lung tissue. Our study thus provides a direct link between a defined cigarette smoke carcinogen and human cancer mutations.

REFERENCES AND NOTES

1. S. S. Hecht, S. G. Carmella, S. E. Murphy, P. G. Foiles, F.-L. Chung, *J. Cell. Biochem. Suppl.* **17F**, 27 (1993).
2. B. Singer and D. Grunberger, *Molecular Biology of Mutagens and Carcinogens* (Plenum, New York, 1983).
3. M. Hollstein, D. Sidransky, B. Vogelstein, C. C. Harris, *Science* **253**, 49 (1991); M. S. Greenblatt, W. P. Bennett, M. Hollstein, C. C. Harris, *Cancer Res.* **54**, 4855 (1994).
4. M. Hollstein *et al.*, *Nucleic Acids Res.* **24**, 141 (1996).

5. E. Eisenstadt, A. J. Warren, J. Porter, D. Atkins, J. H. Miller, *Proc. Natl. Acad. Sci. U.S.A.* **79**, 1945 (1982); M. Mazur and B. Glickman, *Somatic Cell Mol. Genet.* **14**, 393 (1988); R.-H. Chen, V. M. Maher, J. J. McCormick, *Proc. Natl. Acad. Sci. U.S.A.* **87**, 8680 (1990); B. Ruggeri *et al.*, *ibid.* **90**, 1013 (1993).
6. T. Lindahl, *Nature* **362**, 709 (1993).
7. A. J. Levine *et al.*, *Ann. N.Y. Acad. Sci.* **768**, 111 (1995).
8. G. P. Pfeifer, R. Drouin, A. D. Riggs, G. P. Holmquist, *Proc. Natl. Acad. Sci. U.S.A.* **88**, 1374 (1991).
9. HeLa S3 cells (American Type Culture Collection, Rockville, MD) were treated with medium containing 1, 2, or 4 μ M of freshly prepared BPDE (obtained from the National Cancer Institute repository, Midwest Research Institute, Kansas City, MO) for 30 min at 37°C in the dark [S. Venkatachalam, M. Denissenko, A. A. Wani, *Carcinogenesis* **16**, 2029 (1995)]. Controls were treated with solvent only (95% ethanol).
10. A. Sancar and M.-s. Tang, *Photochem. Photobiol.* **57**, 905 (1993); B. Van Houten and A. Snowden, *Bioessays* **15**, 51 (1993).
11. The purified DNA was treated with UvrABC (a 10-fold molar excess of protein over 10⁴ nucleotides of DNA) under standard reaction conditions as described [M.-s. Tang, in *Technologies for Detection of DNA Damage and Mutations*, G. P. Pfeifer, Ed. (Plenum, New York, 1996), pp. 139–153]. After 90 min of incubation at 37°C, the proteins were removed by phenol extractions followed by diethyl ether extraction, and the DNA was purified further by repeated ethanol precipitations. UvrABC nuclease incises six to seven bases 5' and four bases 3' to a BPDE-modified purine, and under these reaction conditions, the cleavage at BPDE-DNA adducts by UvrABC nucleases is quantitative [M.-s. Tang, J. R. Pierce, R. P. Doisy, M. E. Nazimiec, M. C. MacLeod, *Biochemistry* **31**, 8429 (1992)]. These results validate the UvrABC incision method for analysis of the sequence selectivity of BPDE binding. Because the UvrABC incision at the 3' side of BPDE-DNA adducts is very specific (four bases 3' to the adduct), LMPCR can be used to determine the BPDE adduct distribution at nucleotide resolution.
12. UvrABC-induced strand breaks in the *P53* gene were detected by use of LMPCR with *P53*-specific primers [S. Tornaletti, D. Rozek, G. P. Pfeifer, *Oncogene* **8**, 2051 (1993); S. Tornaletti and G. P. Pfeifer, *Science* **263**, 1436 (1994)].
13. S. Tornaletti and G. P. Pfeifer, *Oncogene* **10**, 1493 (1995).
14. Normal human bronchial epithelial cells (Clonetics, San Diego, CA) were cultured in growth medium recommended by the supplier. The cells were treated with 4 μ M of BPDE as described (9).
15. M. F. Denissenko, A. Pao, M.-s. Tang, G. P. Pfeifer, unpublished observations.
16. A. Puisieux, S. Lim, J. Groopman, M. Ozturk, *Cancer Res.* **51**, 6185 (1991).
17. I. Mellon, G. Spivak, P. C. Hanawalt, *Cell* **51**, 241 (1987).
18. R.-H. Chen, V. M. Maher, J. Brouwer, P. van de Putte, J. J. McCormick, *Proc. Natl. Acad. Sci. U.S.A.* **89**, 5413 (1992).
19. Y. Cho, S. Gorina, P. D. Jeffrey, N. P. Pavletich, *Science* **265**, 346 (1994).
20. W. M. Rideout III, G. A. Coetzee, A. F. Olumi, P. A. Jones, *ibid.* **249**, 1288 (1990).
21. We thank S. Bates for cell culture work. Supported by NIH grants CA65652 to G.P.P. and ES03124 to M.-s. T.

29 May 1996; accepted 19 August 1996